Relevance of Relative Sea Surface Temperature for Tropical Rainfall Interannual Variability

Takeshi Izumo, Jérôme Vialard, Matthieu Lengaigne, Iyyappan Suresh

AGU100 ADVANCING EARTH AND SPACE SCIENCE

Geophysical Research Letters

RESEARCH LETTER
10.1029/2019GL086182

Relevance of Relative Sea Surface Temperature for Tropical Rainfall Interannual Variability

Takeshi Izumo[1,2], Jérôme Vialard[1], Matthieu Lengaigne[1,2], and Iyyappan Suresh[3]

[1]Institut de Recherche pour le Développement, Sorbonne Universités (UPMC, Univ Paris 06)-CNRS-IRD-MNHN, LOCEAN Laboratory, IPSL, Paris, France, [2]Formerly also at Indo-French Cell for Water Sciences, IISc-NIO-IITM–IRD Joint International Laboratory, NIO, Goa, India, [3]CSIR-National Institute of Oceanography, Goa, India

Abstract The coupling between sea surface temperature (SST) anomalies and rainfall is an important driver of tropical climate variability. Observations however reveal inconsistencies, such as decreased convective rainfall in regions with positive SST anomalies in the tropical Indian and Atlantic Oceans during and after El Niño–Southern Oscillation (ENSO) events. The upper troposphere warms during El Niño events, stabilizing the atmosphere. SST anomalies only account for the influence of the surface. Using theoretical arguments, we show that relative SST (RSST; defined as SST minus its tropical mean) anomalies, by also accounting for the influence of upper tropospheric temperature anomalies on gross moist stability, explain tropical convection interannual variations better than SST anomalies in observations and climate models. This relation further improves when RSST anomalies are weighted by the precipitation climatology to account for low and high-precipitation regimes. Using RSST is thus essential to understand El Niño–Southern Oscillation teleconnections and interactions between modes of tropical climate variability.

Plain Language Summary Rainfall is an important driver of coupled air-sea climate variability in tropical regions, through its influence on atmospheric motions. Sea surface temperature anomalies influence tropical rainfall, as a warm anomaly is expected to destabilize the atmosphere, yielding a rising motion and increased rainfall. Decreased rainfall however sometimes occurs over positive sea surface temperature anomalies, notably during El Niño events, because these events tend to warm the upper atmosphere in the entire tropics, hence stabilizing the atmosphere and inhibiting rainfall. We show that the relative sea surface temperature, defined as the sea surface temperature minus its average over the tropical oceans, explains precipitation anomalies better than sea surface temperature. Relative sea surface temperature is thus a simple and powerful indicator to better understand year-to-year climate variability, notably El Niño–Southern Oscillation influence on rainfall in the Atlantic and Indian Oceans and its interactions with other tropical ocean-atmosphere coupled modes.

Key Points:
- Relative sea surface temperature (RSST) anomalies are defined as SST anomalies minus their tropical mean
- RSST anomalies, rather than SST anomalies, drive tropical convection interannual variability, especially when weighted by climatological precipitation
- RSST anomalies account for the ENSO-induced upper-tropospheric temperature signal influence on atmospheric stability and explain ENSO teleconnections better

Supporting Information:
- Supporting Information S1

Correspondence to:
T. Izumo,
takeshi.izumo@locean-ipsl.upmc.fr

Citation:
Izumo, T., Vialard, J., Lengaigne, M., & Suresh, I. (2020). Relevance of relative sea surface temperature for tropical rainfall interannual variability. *Geophysical Research Letters*, *47*, e2019GL086182. https://doi.org/10.1029/2019GL086182

Received 13 SEP 2019
Accepted 18 DEC 2019
Accepted article online 30 DEC 2019

1. Introduction

Tropical rainfall variability has strong socioeconomic and environmental impacts, notably in the vulnerable, heavily populated, tropical regions (e.g., Boko et al., 2007; Gadgil & Gadgil, 2006). Convective rainfall, which accounts for most of the tropical rainfall, plays a key role in tropical atmospheric motions. For instance, the latent heat release due to deep-atmospheric convection over the Indo-Pacific warm pool energizes the Walker circulation (e.g., Gill, 1980). A necessary condition for deep atmospheric convection to occur is a sea surface temperature (hereafter, SST) exceeding ~28 °C (e.g., Gadgil et al., 1984; Graham & Barnett, 1987), as it destabilizes the atmosphere. The link between SST and convective interannual anomalies plays a key role in shaping tropical climate variability. During El Niño–Southern Oscillation (ENSO) events, for instance, positive SST anomalies induce enhanced convection in the central Pacific, thereby yielding westerly wind anomalies and an equatorial Pacific oceanic response that will further strengthen the initial SST anomalies. This positive feedback that allows the growth of El Niño events is known as the Bjerknes feedback. It also plays a key role in the development of the Indian Ocean Dipole (IOD; e.g., Saji et al., 1999) and Atlantic Niño (e.g., Merle, 1980), which are intrinsic climate modes in the Indian and Atlantic Oceans, respectively.

This crucial SST-convection relation is however far from perfect, as illustrated in Figure 1. Figure 1a shows the lag-correlation between the El Niño peak intensity and the tropical Indian Ocean SST and rainfall interannual anomalies. The Indian Ocean tends to warm during and after El Niño events, a response to ENSO

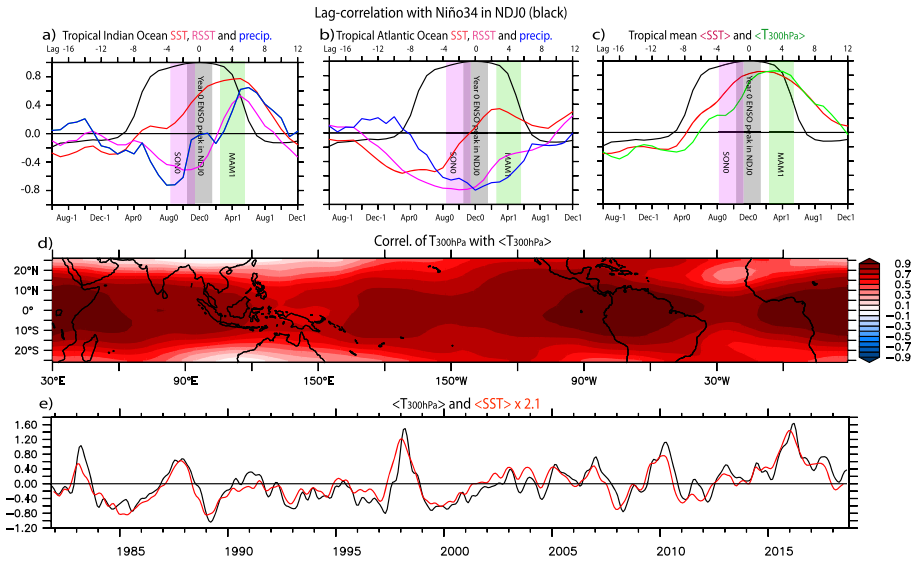

Figure 1. ENSO-induced tropical temperature and precipitation signals. Lag-correlation of Niño3.4 SST anomalies in November–January of year 0 (NDJ0) with anomalies of (a) tropical Indian Ocean (40°E–110°E, 20°N–20°S) mean SST (red), relative SST (RSST; SST minus the tropical mean of SST; cyan) and precipitation (blue), (b) same for tropical Atlantic (70°W–20°E, 20°N–20°S), c) tropical mean 300 hPa (green) and SST (red). The lagged autocorrelation of Niño3.4 with Niño3.4 in NDJ0 is overlaid in black on panels a–c. Vertical shading represents NDJ0, plus the SON0 and MAM1 seasons shown in Figure 3. (d, e) The tropical surface and tropospheric signals during ENSO events. (d) Correlation between 300-hPa temperature anomalies and their tropical mean. (e) Time series of the tropical mean 300-hPa temperature (black; °C) and SST (red; °C) anomalies, relative to the monthly climatology. SST anomalies on panel e have been multiplied by 2.1 (value estimated from a linear regression of the 300-hPa temperature to SST at one month lag, for which the lag correlation is maximum [not shown], as expected from the equatorial adjustment timescale; e.g., Sobel et al., 2002), that is, the 300-hPa temperature anomalies are roughly twice larger than the SST anomalies, because of the condensational heating between the wet surface and dry troposphere along the moist adiabatic (as detailed in the supporting information Text S2). An intraseasonal smoothing has been applied to all fields (details on the methods in the supporting information Text S5).

referred to as the Indian Ocean Basin Mode (IOBM; e.g., Klein et al., 1999) and related "capacitor effect" (Xie et al., 2009). This warming is the result of the eastward shift in the Walker circulation, which induces increased subsidence and downward solar radiation (e.g., Lau & Nath, 2003) and reduced evaporation over the Indian Ocean (e.g., Ohba & Ueda, 2005). This Indian Ocean warming however does not enhance regional rainfall from September to February but rather leads to negligible or negative rainfall anomalies. A similar mismatch between SST and convective anomalies occurs over the Tropical Atlantic. Reduced winds and evaporation also induce a tropical North Atlantic (TNA) warming during the years that follow El Niño events (e.g., García-Serrano et al., 2017), in association with negative rainfall anomalies (Figure 1b). The relation between SST and convective anomalies is hence not always consistent with the simple principle that warmer SST destabilizes the atmosphere and increases rainfall over the tropical Indian and Atlantic Oceans during ENSO events. This mismatch between convective and SST anomalies is likely due to two factors.

First, the atmospheric stability is not only determined by surface properties but also by anomalies in the upper troposphere, as demonstrated by Neelin and Held (1987). Those authors defined gross moist stability (GMS) as the difference of moist static energy (MSE) between the surface and upper troposphere and showed that precipitation (P) tends to be inversely proportional to GMS ($P \approx F/GMS$, F being a constant). Based on partly similar arguments, studies (e.g., Ramsay & Sobel, 2011; Vecchi et al., 2008; Vecchi & Soden, 2007) aimed at understanding the tropical cyclones response to climate change showed that the tropical cyclones potential intensity (PI) rather depends of the *relative* SST (hereafter RSST), defined as the local SST minus its tropical mean (denoted <SST>). The underlying idea is that RSST can be used as a proxy for changes in atmospheric stability (and hence tropical cyclones) in a warming world. Temperature in the upper tropical troposphere is relatively homogenous, due to the fast (~1–2 months) adjustment timescale of equatorial waves in the free atmosphere (e.g., Sobel et al., 2002; Sobel & Bretherton, 2000): this is the commonly

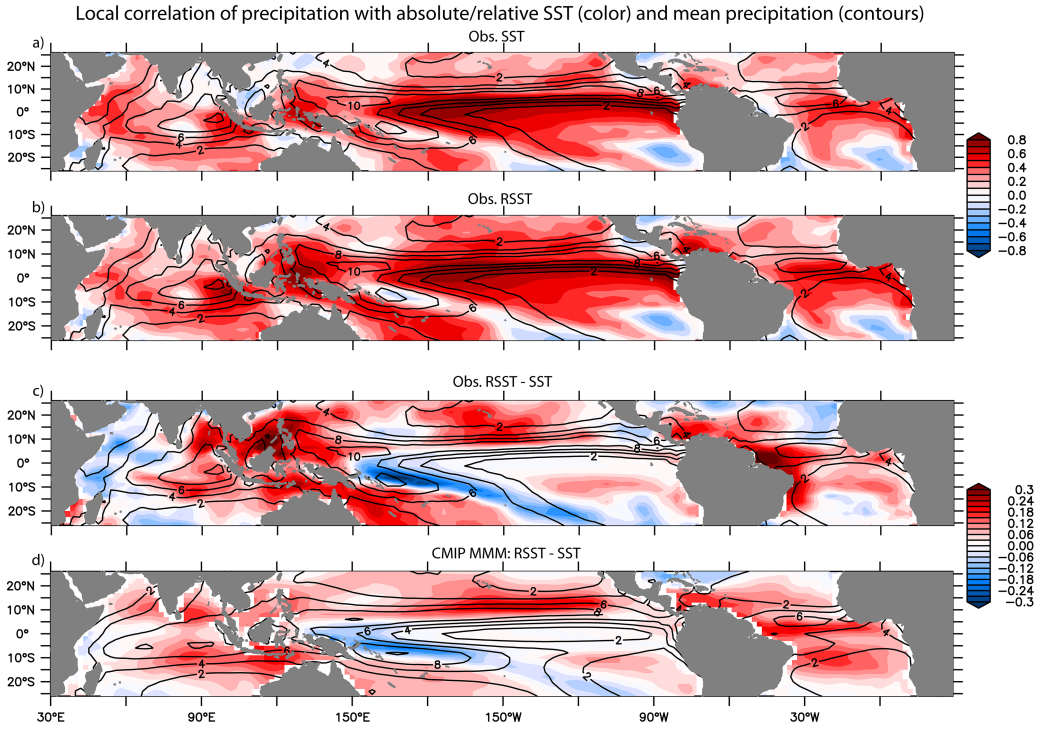

Figure 2. RSST: a more relevant variable for precipitation/deep atmospheric convection interannual variability than SST. Correlation (color) of observed CMAP precipitation anomalies with (a) SST and (b) RSST anomalies. (c) shows (b) minus (a). The precipitation climatology (mm/day) is overlaid as black contours. (d) as (c) but for the multimodel mean (MMM) of 36 CMIP climate models (cf. supporting information Figures S3 and S4 and Text S3). All anomalies have been low-pass filtered using 5-month time and 7.5° longitude, Hanning windows, prior to regression. See supporting information Figure S1 showing that RSST anomalies explain even better observed outgoing longwave radiation (OLR, a proxy of deep atmospheric convection) anomalies.

used weak tropospheric gradient approximation (Ramsay & Sobel, 2011; Sobel et al., 2001). Hence, since the tropical troposphere tends to follow the moist adiabatic vertical profile (e.g., Stone & Carlson, 1979), the upper troposphere will tend to warm uniformly under climate change, so that what matters for changes in atmospheric stability (and hence tropical cyclones) are deviations from the mean surface warming, that is, RSST. Johnson and Xie et al. (2010) used this property to explain that the "threshold" for deep atmospheric convection will increase at the same rate as the tropical mean SST in response to anthropogenic climate change. RSST has to date mostly been used in the global warming context, for instance, to understand the spatial patterns of changes in tropical cyclones (as aforementioned), in the hydrological cycle (e.g., Xie et al., 2010), and to define ENSO events (Williams & Patricola, 2018) and their convective signature (Johnson & Kosaka, 2016) in a warming world. RSST also allows isolating the ENSO and IOD signals in the context of global cooling induced by tropical explosive volcanic eruptions (Izumo et al., 2018; Khodri et al., 2017). RSST is finally useful for characterizing the influence of the equatorial Pacific bias in climate models on the Walker circulation and on ENSO (Bayr et al., 2018, 2019, b). While the above studies largely applied the RSST concept in a global warming/cooling context, Johnson and Xie et al. (2010) remarked that it also seems to explain year-to-year variations of the SST threshold for tropical convection in the Coupled Model Intercomparison Project (CMIP) database (cf. discussion of their Figure 2b). This suggests that the RSST concept can also be used to account for the effect of variations in upper tropospheric temperature on stability at the interannual timescale. The entire tropical troposphere indeed tends to warm (cool) during and after El Niño (La Niña) events (Figures 1c–1e), increasing (decreasing) the atmospheric stability. The better agreement in Figures 1a and 1b between the Indian Ocean or Atlantic basin-averaged precipitation and RSST anomalies, than with SST anomalies, suggest that the RSST concept can also be used at the interannual timescale. Our first objective in this paper is to formally show why RSST anomalies control atmospheric stability at interannual timescale (section 2) and to demonstrate that precipitation and convection interannual anomalies are better explained by RSST anomalies than by SST anomalies (section 4).

A second possible cause for mismatches between SST and rainfall anomalies, for example, in Figure 1ab, is the nonlinearity of the SST-precipitation relationship. As already noted, tropical deep convection indeed occurs above ~28 °C in the present climate (e.g., Gadgil et al., 1984; Jauregui & Takahashi, 2018). This implies that SST variations mostly influence rainfall in climatologically high SST regions (e.g., He et al., 2018). Previous studies (Flannaghan et al., 2014; Fueglistaler et al., 2015; Sobel et al., 2002) have defined a tropical mean precipitation-weighted (or rainy) SST to take this effect into account. The simple idea is to give more weight to SST anomalies in regions where it rains more. Because we aim at explaining local rainfall anomalies, our second objective in this paper will be to test if a weighting of the RSST anomalies by the precipitation climatology further improves their agreement with precipitation/convection anomalies by implicitly accounting for the climatological SST and precipitation distribution.

In section 2, we develop theoretical arguments to explain why RSST anomalies should be a proxy of interannual precipitation anomalies, especially when weighted by climatological precipitation. In section 3, we briefly present the data and methods used (described in detail in the supporting information Text S5). In section 4, we first demonstrate that RSST anomalies better explain tropical precipitation anomalies than SST anomalies, because they integrate the effect of the upper-tropospheric temperature anomalies on the atmospheric stability, in particular in the Atlantic and Indian Oceans and around the maritime continent during ENSO events. We then define a climatological precipitation-weighted RSST (PcRSST) anomalies and show that it performs even better for explaining anomalous precipitation patterns. We discuss our results—strengthened by analyses of 36 CMIP models in the supporting information—in section 5, including implications for a better understanding of interactions between modes of tropical climate variability.

2. RSST as a Proxy of Atmospheric Stability

Here we summarize the main steps of our theoretical demonstration explaining why GMS and precipitation interannual anomalies $P'(P' = P-\overline{P}$, with the overbar denoting the seasonal cycle and the prime denoting the anomaly relative to the seasonal cycle) respond to RSST anomalies (see supporting information Texts S1 and S2 for a complete derivation and more thorough discussion of the approximations involved). GMS is defined as follows:

$$\mathrm{GMS} = m_t - m_s$$

where the t and s subscripts respectively denote the upper troposphere (300 hPa level; e.g., Fueglistaler et al., 2015) and surface, m is the MSE, $m = s+L_v q = C_p T+gz+L_v q$, where s is the dry static energy, L_v the latent heat of vaporization, q the specific humidity, C_p the specific heat at constant pressure, T the temperature, g the gravitational constant, and z the altitude. The tropical atmosphere approximately follows the moist adiabatic lapse rate (Stone & Carlson, 1979), so that $<m_t>' = <m_s>'$, where $<>$ denotes the 20°N–20°S tropical mean (cf. supporting information Text S5A discussing this choice). The upper troposphere is almost dry, and its MSE hence mainly depends on *temperature*: $m_t \approx s_t = C_p T_t+gz_t \approx (C_p+R/M_{air})\, T_t$, where R is the ideal gas constant and M_{air} the air molar mass. Finally, T_t' is rather uniform across the tropical band (weak tropospheric gradient approximation; Sobel et al., 2001), so that $m_t' \approx <m_t>'$. Given all these approximations, the GMS anomalies are given by $GMS' \approx <m_s'> - m_s'$.

If we assume an almost constant relative humidity (typically around 80% in the tropics) and a 7% change in specific humidity q_s per °C of SST change (linearization of Clausius-Clapeyron), then $m_s' = C_p\, T_s' + L_v\, q_s' \approx (C_p + 0.07\, L_v\, \overline{q}_s)\, T_s'$, that is, surface MSE' is proportional to SST'. Therefore, to the first order, $GMS' \approx (C_p + 0.07\, L_v\, \overline{q}_s)(<T_s'> - T_s')$. As $RSST' = T_s' - <T_s'>$, we obtain

$$\mathrm{GMS}' \approx -(\mathrm{C_p} + 0.07\, \mathrm{L_v}\, \overline{\mathrm{q}}_\mathrm{s})\ \mathrm{RSST}'$$

Finally, exploiting the theoretical relation between GMS and precipitation derived by Neelin and Held (1987), we obtain

$$P' \approx \mathrm{RSST}'\ \overline{P}\ \left(C_p + 0.07\, L_v\, \overline{q}_s\right) / \overline{\mathrm{GMS}}$$

That is, precipitation interannual anomalies should be proportional to RSST anomalies. The proportionality constant depends of the climatological mean state and is in particular proportional to $\overline{P}$ and, hence, expected to be larger in regions of high climatological precipitation and SST.

In this section, we have shown that RSST anomalies should be a proxy of tropical precipitation interannual anomalies, especially if weighted by climatological precipitation. This derivation nonetheless involved several strong approximations (for instance the upper tropospheric signal is not completely homogeneous; Figure 1d). Section 4 will however demonstrate that RSST anomalies and Pc-RSST anomalies explain indeed well tropical precipitation and convection interannual anomalies, better than SST anomalies, hence justifying our strong assumptions a posteriori.

3. Data and Methods

We only give a brief summary of our data and methods here, with a comprehensive description in the supporting information. We use the OISSTv2 SST product (Reynolds et al., 2002), NCEP2 reanalysis (Kanamitsu et al., 2002) for temperature at 300 hPa and NOAA Climate Data Record Outgoing Longwave Radiation (CDR OLR; Hai-Tien Lee and NOAA Climate Data Record Program, 2018) as a proxy for deep atmospheric convection and CMAP1 precipitation (Xie & Arkin, 1997). All the analyses are performed on monthly anomalies relative to the mean monthly seasonal cycle, over the November 1981 to 2018 period. The anomalies are smoothed to remove unwanted intraseasonal frequencies prior to analysis. The results are robust when no detrending or smoothing is applied (cf. supporting information Figure S2). We use classical indices of the interannual tropical climate variability, based on average SST anomalies: the Niño3.4 index for ENSO, Dipole Mode Index (DMI) for the IOD, and the Atl3 index for the Atlantic Niño.

4. Results

Figure 2a shows the correlation between precipitation and local SST anomalies. There is a positive correlation, often above 0.4 (and up to above 0.8 in the central equatorial Pacific), in most rainy regions in the tropics, illustrating the tendency for positive SST anomalies to destabilize the atmosphere and hence to induce more convective rainfall (and vice versa for negative SST anomalies). This relation is particularly strong in the central equatorial Pacific and on the southern flank of the Pacific intertropical convergence zone (ITCZ) due to the strong ENSO signal there. This relationship illustrates the response of atmospheric deep convection to SST anomalies (e.g., Gadgil et al., 1984; Graham & Barnett, 1987) at timescales longer than the intraseasonal one, except in dry, subsident regions where cloud negative radiative feedbacks can dominate (e.g., He et al., 2018). Overall, SST anomalies hence explain a significant part of the deep convection interannual variability in tropical rainy regions.

Our first objective in this paper is to test the added value of using RSST to explain tropical convection interannual variability. Figure 2b shows the same analysis as Figure 2a but based on RSST anomalies, and panel c shows the differences between the two panels. This figure indicates that RSST anomalies better explain convection interannual variability over tropical rainy regions than SST anomalies. This improvement is particularly evident over the warm-pool areas, that is, over the western equatorial Atlantic, the central and eastern equatorial Indian Ocean, the maritime continent, and the western Pacific where correlation increases by up to ~0.35 (Figure 2c). The improvement is even better (up to ~0.5) when using a deep atmospheric convection proxy (Outgoing Longwave Radiation; supporting information Figure S1), better observed than precipitation. A qualitativelysimilar improvement is also evident when performing similar analyses in the CMIP5 (Intergovernmental Panel on Climate Change; IPCC, 2013) database (with obviously some differences related notably to models typical climatological biases; Figure 2d and supporting information Figures S3 and S4 and Texts S3 and S4). Conversely, RSST anomalies do not perform better than SST anomalies to explain rainfall interannual variations over the central and eastern equatorial Pacific.

Let us now discuss the reasons for this improved performance of RSST anomalies. As mentioned earlier, RSST anomalies encapsulate the effect of the upper tropospheric temperature anomalies on gross moist stability, while SST anomalies do not. Those upper tropospheric temperature anomalies are quite uniform across the tropical band (Figure 1d) and are strongly correlated to the tropical-mean SST anomaly (Figures 1c and 1e) and to the ENSO signal with a 1- to 2-month time lag (Figure 1c). The tropical mean SST component of the RSST expression hence largely captures the stabilizing (destabilizing) effect of the upper tropospheric warming (cooling) on the atmosphere during El Niño (La Niña) events. In the Pacific, this effect is small relative to the much larger effect of local SST anomalies. This explains the similar performance of SST and RSST anomalies in the central and eastern Pacific regions. The northern half of the South

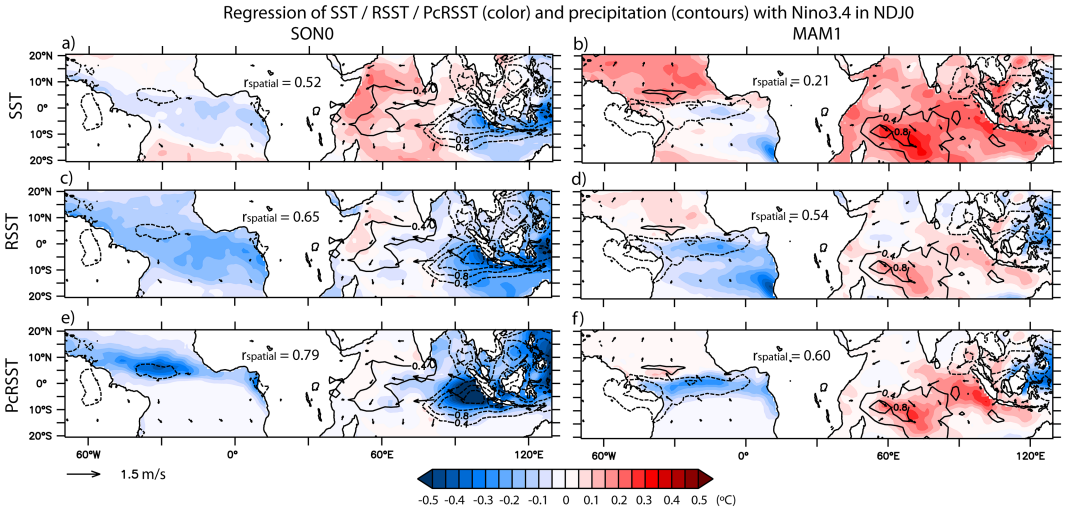

Figure 3. RSST anomalies explain ENSO remote influences on precipitation better than SST anomalies. Seasonally stratified regression of September–November (SON0) averaged (a) SST anomalies (^{o}C), (c) RSST anomalies (^{o}C), and (e) Climatological precipitation-weighted RSST (PcRSST; ^{o}C) anomalies (color) on the following November to January (NDJ0) Niño3.4 index (normalized by its standard deviation, so that the regression slope illustrates typical amplitudes in physical units). Precipitation (contours; mm day^{-1}) and surface wind (vectors, when significant at the 90% level; at 10 m; m s^{-1}) anomalies are overlaid. (b–d): Same as a, c, and e but for March to May (MAM1) averaged anomalies regressed onto the preceding November to January (NDJ0) Niño3.4 index. The values of the uncentered spatial pattern correlations ($r_{spatial}$) between precipitation and SST, RSST, or PcSST anomalies are indicated on each panel: PcRSST anomalies explain the precipitation anomalies best, followed by RSST anomalies.

Pacific Convergence Zone is the only region showing a slightly degraded performance of RSST anomalies (Figure 2c-d and supporting information Figure S1), most likely because ENSO-related circulation anomalies (e.g., Vincent et al., 2011) also influence rainfall in this region. On the other hand, the improved performance of RSST anomalies over the Indian and Atlantic oceans and maritime continent suggests that the ENSO-induced tropospheric temperature signals play a relatively strong role in controlling the atmospheric stability interannual variations there. Below, we examine this by investigating the ENSO teleconnection patterns to the Atlantic and Indian Oceans in terms of SST, RSST, and precipitation anomalies (Figures 3a–3d).

For ENSO-related SST anomalies, in boreal fall (September to November) prior to an El Niño peak, there is a marked IOD signal in the Indian Ocean (Figure 3a), due to the tendency of the IOD to phase-lock to ENSO (e.g., Annamalai et al., 2003; Ohba & Ueda, 2005). By the following spring (March to May), the IOD signal is replaced by a clear IOBM warming signal (Figure 3b). In the Atlantic, the weak Atlantic Niña tendency in fall (Figure 3a) progressively evolves into a Tropical North Atlantic warming (Figure 3b), which peaks the following spring (e.g., Taschetto et al., 2016). However, these Indo-Atlantic SST anomalies do not match the observed pattern of precipitation anomalies well (Figures 3a and 3b). The Indo-Atlantic uncentered pattern correlation between ENSO-related precipitation and SST anomalies is only 0.52 in fall (Figure 3a) and 0.21 in the following spring (Figure 3b). For instance, in the Indian Ocean, positive SST anomalies in the Bay of Bengal are associated with negative precipitation anomalies. Notably, in boreal fall, these negative precipitation anomalies are much broader than the underlying negative SST anomalies of the IOD east pole, which are relatively weak and confined. In the Atlantic, there are significant negative rainfall anomalies along the ITCZ in spring, in the absence of clear negative SST anomalies (Figure 3b).

RSST anomalies are negatively offset relative to SST anomalies during an El Niño (Figures 3c and 3d) due to the removal of the positive tropical mean SST anomaly (Figure 1). This offset captures the stabilizing effect of the upper tropospheric warming over the Atlantic and Indian Oceans during El Niño events that tends to hinder precipitation. As a result, the spatial patterns of precipitation anomalies match those of RSST anomalies better than those of SST anomalies. Pattern correlations indeed increase from 0.52 to 0.65 in fall (Figures 3a and 3c), from 0.21 to 0.54 in the following spring (Figures 3b and 3d), and even from −0.02 to +0.52 in winter (supporting information Figure S5). The decreased rainfall over the Bay of Bengal, increased rainfall in the southwestern Indian Ocean in spring, or decreased rainfall along the Atlantic ITCZ all match the RSST pattern better than that of SST. RSST not only explains precipitation anomalies better than SST, but

also explains better the near surface wind anomalies that precipitation anomalies induce. For instance, the correlation between the DMI eastern pole index (when using RSST instead of SST) and equatorial Indian Ocean zonal windstress anomalies (in boreal fall during IOD peak season) increase from 0.68 to 0.83 or that between the Atl3 index and equatorial Atlantic zonal windstress (in spring–summer during Atlantic Niño peak season) from 0.8 to 0.89 (both improvements being significant at the 95% confidence level). Overall, this illustrates that the effect of ENSO on upper tropospheric temperature needs to be considered in addition to local SST anomalies to explain the rainfall and surface wind interannual anomalies in the tropical Indian and Atlantic oceans.

Even though RSST anomalies exhibit a better pattern agreement with precipitation anomalies than SST anomalies, the agreement can be further improved. For instance, dry anomalies above the IOD eastern pole only extend down to 10°S, while the broad negative RSST anomalies extend farther south (Figure 3c). Similarly, the Atlantic exhibits a very broad tropical negative RSST anomalies, while the rainfall decrease is confined near the equator, notably in the west Atlantic and neighbouring South America. In both cases, the precipitation anomalies tend to be more concentrated in the regions of highest climatological SST and rainfall. This brings us to our second objective: to test the potential added value of weighting RSST anomalies by the precipitation climatology to better explain convective precipitation interannual variability. We define $PcRSST' = Pc \times RSST' / <Pc>$, where Pc is the monthly precipitation climatology. The spatial patterns of PcSST anomalies even better match those of rainfall anomalies both in fall, notably in the eastern Indian Ocean and Atlantic (Figure 3e), and spring (Figure 3f). The IOD in fall is actually rather an east IO "monopole" than a dipole in terms of PcRSST and precipitation, and the Atlantic meridional dipole in spring as well is almost an equatorial monopole. This better match results in an Indo-Atlantic pattern correlation improvement from 0.65 to 0.79 in fall and 0.54 to 0.60 in the following spring. PcRSST anomalies are also very relevant during the ENSO peak in winter, improving the Indo-Pacific pattern correlation from 0.52 to 0.67 (supporting information Figure S5). As a comparison, using SST weighted by precipitation climatology, PcSST, leads only to a slight improvement as compared to SST, weaker than RSST, and hence clearly weaker than PcRSST (not shown). Furthermore, El Niño and La Niña composites equivalent to Figure 3 confirm that Pc-RSST and RSST match Indian Ocean and Atlantic precipitation anomalies better than SST for both ENSO phases (supporting information Figures S6 and S7), that is, that the nonlinear relation between surface temperature and precipitation does not affect the superior performance of RSST.

Overall, this analysis demonstrates that PcRSST can explain very well (and thus is a very good proxy of) the precipitation interannual anomalies over the Indian and Atlantic oceans, because it encapsulates both the surface and the upper tropospheric influences on atmospheric stability and takes into account some of the non-linear dependency of rainfall to SST, with the strongest rainfall response at high SST.

5. Discussion

Earlier studies have introduced RSST (simply defined as SST minus its tropical mean) as a driver of the changes in tropical cyclones and tropical atmospheric deep convection/precipitation in the context of climate change. Using a theoretical derivation, we show that precipitation interannual anomalies should also be proportional to RSST interannual anomalies, with a larger proportionality coefficient in climatologically high rainfall regions. Using observations—and CMIP models (see also supporting information)—we show that RSST anomalies explain deep atmospheric convection anomalies better than SST anomalies do, because RSST anomalies encapsulate the effects of upper-tropospheric temperature anomalies on stability changes. This is particularly relevant during ENSO events, because El Niño (La Niña) uniformly warms (cools) the upper troposphere, thereby stabilizing (destabilizing) the tropical atmosphere. In CMIP models, this added value of RSST is thus larger in the models having larger ENSO amplitude (supporting information Figure S4) and is projected to remain robust in the future (supporting information Texts S3 and S4) .

Weighting RSST anomalies by the precipitation climatology (PcRSST) further improves the consistency with interannual rainfall anomalies, by accounting for the nonlinearity in the SST-rainfall relation, with tropical rainfall mostly occurring above a SST threshold of ~28 °C in the current climate (i.e., above a RSST threshold of ~1 °C; Johnson & Xie, 2010). PcRSST can also help us in understanding the asymmetries of El Niño and La Niña teleconnections (supporting information Figures S6 and S7). RSST anomalies/PcRSST anomalies are thus easy-to-compute, physical variables (and thus proxies) driving tropical precipitation/convection

anomalies (and their dynamical response, notably surface wind). They account both for the effects of surface and upper-tropospheric temperature anomalies, for example, in the context of the pan-tropical upper tropospheric signals induced by ENSO but also in those associated with global climate change (e.g., Johnson & Xie, 2010; Vecchi et al., 2008; Vecchi & Soden, 2007) or tropical explosive volcanic eruptions (Khodri et al., 2017). RSST should thus be used, instead of SST (or at least complementary to SST), to define coupled climate modes indices (e.g., Atl3, DMI east pole and Niño3.4 RSST) that are more dynamically consistent with precipitation/wind. Such RSST use should become even more essential in the increasing warming trend context due to global anthropogenic warming (supporting information Text S4).

Our results have implications for the studies that investigate remote effects of SST anomalies (in, for example, the Atlantic or Indian Ocean) on the evolution of ENSO events, both at interannual and decadal timescales (RSST concept being a priori valid for both). Such studies often investigate teleconnections to winds over the Pacific using atmospheric (or coupled) general circulation models sensitivity experiments forced by SST anomalies applied only in the Atlantic or Indian Ocean for example (e.g., Annamalai et al., 2005; Chikamoto, 2014; Dayan et al., 2015; Ding et al., 2012; Ham et al., 2013; Luo et al., 2012; McGregor et al., 2014; Santoso et al., 2012). While this strategy is correct for SST anomalies that are independent of ENSO, it may give a biased result for climate modes that are tightly associated with ENSO. The IOBM and TNA are for instance systematically forced by an ENSO signal and will hence always be associated to an upper tropospheric temperature signal. A numerical experiment forced by SST anomalies only applied in the Indian Ocean or Atlantic will miss most of the upper tropospheric signal and, hence, not accurately estimate the actual regional precipitation anomalies and their remote circulation response over the Pacific. In other words, since RSST anomalies explain precipitation (and wind) anomalies related to tropical climate coupled modes (for example, the IOD, the IOBM, and TNA) better than SST anomalies (Figure 3), it would be more appropriate to apply RSST rather than SST anomalies in the Atlantic and Indian oceans, in such numerical sensitivity experiment, to study their remote effects on the Pacific.

RSST could also allow revisiting interactions between tropical climate modes (e.g., Cai et al., 2019). Many studies have for instance questioned the interdecadal stability of the ENSO influence on tropical Atlantic SST (e.g., Ding et al., 2012; RodríguezFonseca et al., 2009). The correlation between Niño3.4 and Atl3 SST anomalies in April–June (Atlantic Niño peak season) is indeed significant at the 95% level over the 1981–2001 period ($r = 0.58$) but not over 1998–2018 ($r = 0.39$). This correlation is significant over both periods when computed from RSST anomalies (0.70 and 0.59; in fact, there is a more robust correlation using RSST anomalies over the entire historical period). This suggests that the remote influence of ENSO on Atlantic rainfall and the associated wind anomalies (i.e., the ENSO teleconnection to the Atlantic) has remained quite stable over recent decades. What has not remained stable is the tendency of this atmospheric circulation change to induce an SST anomaly (Chang et al., 2006). This provides new clues to investigate the relations between ENSO and the Atlantic. Similarly, additional analyses based on RSST anomalies (not shown) highlight the dominant role of the IOD eastern pole (actually a RSST monopole; Figures 3, S5, and S6) in generating a rainfall response over the IO and related wind responses over the equatorial IO and western Pacific. The RSST anomalies hence offer interesting perspectives to study the IOD influence on ENSO (e.g., Izumo et al., 2010, 2013, 2016; Jourdain et al., 2016; Wieners et al., 2017).

Acknowledgments
We thank the two reviewers, Thomas Bayr and an anonymous one, for their constructive comments on this work. We thank Institut de Recherche pour le Développement (IRD) and CSIR-National Institute of Oceanography (CSIR-NIO) for their continuous supports. This work was mainly done while TI was a visiting scientist under IRD funding at CSIR-NIO. J. V. thanks IRD for funding regular visits to CSIR-NIO and CSIR-NIO for his "Adjunct Scientist" position. This work has also been funded by the ARISE ANR (Agence Nationale pour la Recherche) project (ANR-18-CE01-0012). This is NIO contribution 6481. We thank NOAA for making the FERRET software available. Data sets for this research are included in this paper, cf. references cited in section 3.

References

Annamalai, H., Murtugudde, R., Potemra, J., Xie, S. P., Liu, P., & Wang, B. (2003). Coupled dynamics over the Indian Ocean: Spring initiation of the zonal mode. *Deep Sea Research Part II: Topical Studies in Oceanography*, *50*(12-13), 2305–2330. https://doi.org/10.1016/S0967-0645(03)00058-4

Annamalai, H. S. P. X., Xie, S. P., McCreary, J. P., & Murtugudde, R. (2005). Impact of Indian Ocean sea surface temperature on developing El Niño. *Journal of Climate*, *18*(2), 302–319. https://doi.org/10.1175/JCLI-3268.1

Bayr, T., Domeisen, D. I. V., & Wengel, C. (2019). The effect of the equatorial Pacific cold SST bias on simulated ENSO teleconnections to the North Pacific and California. *Climate Dynamics*, *53*(7-8), 3771–3789. https://doi.org/10.1007/s00382-019-04746-9

Bayr, T., Latif, M., Dommenget, D., Wengel, C., Harlaß, J., & Park, W. (2018). Mean-state dependence of ENSO atmospheric feedbacks in climate models. *Climate Dynamics*, *50*(9-10), 3171–3194. https://doi.org/10.1007/s00382-017-3799-2

Bayr, T., Wengel, C., Latif, M., Dommenget, D., Lübbecke, J., & Park, W. (2019). Error compensation of ENSO atmospheric feedbacks in climate models and its influence on simulated ENSO dynamics. *Climate Dynamics*, *53*(1-2), 155–172. https://doi.org/10.1007/s00382-018-4575-7

Boko, M., Niang, I., Nyong, A., Vogel, C., Githeko, A., Medany, M., et al. (2007). Africa. In M. L. Parry, O. F. Canziani, J. P. Palutikof, P. J. van der Linden, & C. E. Hanson (Eds.), *Climate change 2007: Impacts, adaptation and vulnerability. contribution of working group II to the fourth assessment report of the intergovernmental panel on climate change* (pp. 433–467). Cambridge UK: Cambridge University Press.

Cai, W., Wu, L., Lengaigne, M., Li, T., McGregor, S., Kug, J. S., & Ham, Y. G. (2019). Pantropical climate interactions. *Science*, *363*(6430), eaav4236. https://doi.org/10.1126/science.aav4236

Chang, P., Fang, Y., Saravanan, R., Ji, L., & Seidel, H. (2006). The cause of the fragile relationship between the Pacific El Niño and the Atlantic Niño. *Nature*, *443*(7109), 324–328. https://doi.org/10.1038/nature05053

Chikamoto, Y. (2014). Recent Walker circulation strengthening and Pacific cooling amplified by Atlantic warming. *Nature Climate Change*, *4*(10), 888. https://doi.org/10.1038/nclimate2330

Dayan, H., Izumo, T., Vialard, J., Lengaigne, M., & Masson, S. (2015). Do regions outside the tropical Pacific influence ENSO through atmospheric teleconnections? *Climate Dynamics*, *45*(3-4), 583–601. https://doi.org/10.1007/s00382-014-2254-x

Ding, H., Keenlyside, N. S., & Latif, M. (2012). Impact of the equatorial Atlantic on the El Niño southern oscillation. *Climate Dynamics*, *38*(9-10), 1965–1972. https://doi.org/10.1007/s00382-011-1097-y

Flannaghan, T. J., Fueglistaler, S., Held, I. M., Po-Chedley, S., Wyman, B., & Zhao, M. (2014). Tropical temperature trends in atmospheric general circulation model simulations and the impact of uncertainties in observed SSTs. *Journal of Geophysical Research-Atmospheres*, *119*(23), 13–327. https://doi.org/10.1002/2014jd022365

Fueglistaler, S., Radley, C., & Held, I. M. (2015). The distribution of precipitation and the spread in tropical upper tropospheric temperature trends in CMIP5/AMIP simulations. *Geophysical Research Letters*, *42*(14), 6000–6007. https://doi.org/10.1002/2015GL064966

Gadgil, S., & Gadgil, S. (2006). The Indian monsoon, GDP and agriculture. *Economic and Political Weekly*, 4887–4895.

Gadgil, S., Joseph, V., & Joshi, N. V. (1984). Ocean-atmosphere coupling over monsoon regions. *Nature*, *312*(5990), 141–143. https://doi.org/10.1038/312141a0

García-Serrano, J., Cassou, C., Douville, H., Giannini, A., & Doblas-Reyes, F. J. (2017). Revisiting the ENSO teleconnection to the tropical North Atlantic. *Journal of Climate*, *30*(17), 6945–6957. https://doi.org/10.1175/JCLI-D-16-0641.1

Gill, A. E. (1980). Some simple solutions for heat-induced tropical circulation. *Quarterly Journal of the Royal Meteorological Society*, *106*(449), 447–462. https://doi.org/10.1002/qj.49710644905

Graham, N. E., & Barnett, T. P. (1987). Sea surface temperature, surface wind divergence, and convection over tropical oceans. *Science*, *238*(4827), 657–659. https://doi.org/10.1126/science.238.4827.657

Ham, Y. G., Kug, J. S., Park, J. Y., & Jin, F. F. (2013). Sea surface temperature in the north tropical Atlantic as a trigger for El Niño/Southern Oscillation events. *Nature Geoscience*, *6*(2), 112–116. https://doi.org/10.1038/ngeo1686

He, J., Johnson, N. C., Vecchi, G. A., Kirtman, B., Wittenberg, A. T., & Sturm, S. (2018). Precipitation sensitivity to local variations in tropical sea surface temperature. *Journal of Climate*, *31*(22), 9225–9238. https://doi.org/10.1175/JCLI-D-18-0262.1

IPCC (2013). In T. F. Stocker, D. Qin, G.-K. Plattner, M. Tignor, S. K. Allen, J. Boschung, A. Nauels, Y. Xia, V. Bex, & P. M. Midgley (Eds.), *Climate change 2013: The physical science basis. Contribution of Working Group I to the Fifth Assessment Report of the Intergovernmental Panel on Climate Change*, (p. 1535). Cambridge, United Kingdom and New York, NY, USA: Cambridge University Press.

Izumo, T., Khodri, M., Lengaigne, M., & Suresh, I. (2018). A subsurface Indian Ocean dipole response to tropical volcanic eruptions. *Geophysical Research Letters*, *45*(17), 9150–9159. https://doi.org/10.1029/2018GL078515

Izumo, T., Lengaigne, M., Vialard, J., Luo, J. J., Yamagata, T., & Madec, G. (2013). Influence of Indian Ocean Dipole and Pacific recharge on following year's El Niño: Interdecadal robustness. *Climate Dynamics*, *42*(1-2), 291–310. https://doi.org/10.1007/s00382-012-1628-1

Izumo, T., Vialard, J., Dayan, H., Lengaigne, M., & Suresh, I. (2016). A simple estimation of equatorial Pacific response from wind stress to untangle Indian Ocean Dipole and Basin influences on El Niño. *Climate Dynamics*, *46*(7-8), 2247–2268. https://doi.org/10.1007/s00382-015-2700-4

Izumo, T., Vialard, J., Lengaigne, M., de Boyer Montegut, C., Behera, S. K., Luo, J. J., & Yamagata, T. (2010). Influence of the state of the Indian Ocean Dipole on the following year's El Niño. *Nature Geoscience*, *3*(3), 168–172. https://doi.org/10.1038/ngeo760

Jauregui, Y. R., & Takahashi, K. (2018). Simple physical-empirical model of the precipitation distribution based on a tropical sea surface temperature threshold and the effects of climate change. *Climate Dynamics*, *50*(5-6), 2217–2237. https://doi.org/10.1007/s00382-017-3745-3

Johnson, N. C., & Kosaka, Y. (2016). The impact of eastern equatorial Pacific convection on the diversity of boreal winter El Niño teleconnection patterns. *Climate Dynamics*, *47*(12), 3737–3765. https://doi.org/10.1007/s00382-016-3039-1

Johnson, N. C., & Xie, S.-P. (2010). Changes in the sea surface temperature threshold for tropical convection. *Nature Geoscience*, *3*(12), 842–845. https://doi.org/10.1038/ngeo1008

Jourdain, N. C., Lengaigne, M., Vialard, J., Izumo, T., & Gupta, A. S. (2016). Further insights on the influence of the Indian Ocean dipole on the following year's ENSO from observations and CMIP5 models. *Journal of Climate*, *29*(2), 637–658. https://doi.org/10.1175/JCLI-D-15-0481.1

Kanamitsu, M., W. Ebisuzaki, J. Woollen, S-K Yang, J.J. Hnilo, M. Fiorino, and G. L. Potter. NCEP-DOE AMIP-II Reanalysis (R-2). 1631-1644, *Bulletin of the American Meteorological Society*. Nov 2002, *83*, 11, DOI: https://doi.org/10.1175/BAMS-83-11-1631,

Khodri, M., Izumo, T., Vialard, J., Janicot, S., Cassou, C., Lengaigne, M., & Robock, A. (2017). Tropical explosive volcanic eruptions can trigger El Niño by cooling tropical Africa. *Nature Communications*, *8*(1), 778. https://doi.org/10.1038/s41467-017-00755-6

Klein, S. A., Soden, B. J., & Lau, N. C. (1999). Remote sea surface temperature variations during ENSO: Evidence for a tropical atmospheric bridge. *Journal of Climate*, *12*(4), 917–932. https://doi.org/10.1175/1520-0442(1999)012<0917:RSSTVD>2.0.CO;2

Lau, N. C., & Nath, M. J. (2003). Atmosphere-ocean variations in the Indo-Pacific sector during ENSO episodes. *Journal of Climate*, *16*(1), 3–20. https://doi.org/10.1175/1520-0442(2003)016<0003:AOVITI>2.0.CO;2

Hai-Tien Lee and NOAA CDR Program (2018): NOAA Climate Data Record (CDR) of Monthly Outgoing Longwave Radiation (OLR), Version 2.7. NOAA National Centers for Environmental Information. https://doi.org/10.7289/V5W37TKD

Luo, J. J., Sasaki, W., & Masumoto, Y. (2012). Indian Ocean warming modulates Pacific climate change. *Proceedings of the National Academy of Sciences*, *109*(46), 18,701–18,706. https://doi.org/10.1073/pnas.1210239109

McGregor, S., Timmermann, A., Stuecker, M. F., England, M. H., Merrifield, M., Jin, F. F., & Chikamoto, Y. (2014). Recent Walker circulation strengthening and Pacific cooling amplified by Atlantic warming. *Nature Climate Change*, *4*(10), 888–892. https://doi.org/10.1038/nclimate2330

Merle, J. (1980). Variabilite thermique annuelle et interannuelle de l'Océan Atlantique équatorial Est: L'hypothese d'un “El Niño” Atlantique, Oceanol. *Oceanologica Acta*, *3*, 209–220.

Neelin, J. D., and I. M. Held, 1987: Modeling tropical convergence based on the moist static energy budget. *Monthly Weather Review*, *115*, 3–12, https://doi.org/10.1175/1520-0493(1987)115,0003:MTCBOT.2.0.CO;2,1

Ohba, M., & Ueda, H. (2005). Basin-wide warming in the equatorial Indian Ocean associated with El Niño. *SOLA*, *1*, 89–92. https://doi.org/10.2151/sola

Ramsay, H. A., & Sobel, A. H. (2011). Effects of relative and absolute sea surface temperature on tropical cyclone potential intensity using a single-column model. *Journal of Climate*, *24*(1), 183–193. https://doi.org/10.1175/2010JCLI3690.1

Reynolds, R. W., Rayner, N. A., Smith, T. M., Stokes, D. C., & Wang, W. (2002). An improved in situ and satellite SST analysis for climate. *Journal of Climate*, *15*(13), 1609–1625. https://doi.org/10.1175/1520-0442(2002)015<1609:AIISAS>2.0.CO;2

RodríguezFonseca, B., Polo, I., García-Serrano, J., Losada, T., Mohino, E., Mechoso, C. R., & Kucharski, F. (2009). Are Atlantic Niño's enhancing Pacific ENSO events in recent decades? *Geophysical Research Letters*, *36*(20). https://doi.org/10.1029/2009gl040048

Saji, N. H., Goswami, B. N., Vinayachandran, P. N., & Yamagata, T. (1999). A dipole mode in the tropical Indian Ocean. *Nature*, *401*(6751), 360–363. https://doi.org/10.1038/43854

Santoso, A., England, M. H., & Cai, W. (2012). Impact of Indo-Pacific feedback interactions on ENSO dynamics diagnosed using ensemble climate simulations. *Journal of Climate*, *25*(21), 7743–7763. https://doi.org/10.1175/JCLI-D-11-00287.1

Sobel, A. H., & Bretherton, C. S. (2000). Modeling tropical precipitation in a single column. *Journal of Climate*, *13*(24), 4378–4392. https://doi.org/10.1175/1520-0442(2000)013<4378:MTPIAS>2.0.CO;2

Sobel, A. H., Held, I. M., & Bretherton, C. S. (2002). The ENSO signal in tropical 70 tropospheric temperature. *Journal of Climate*, *15*(18), 2702–2706. https://doi.org/10.1175/1520-0442(2002)015<2702:TESITT>2.0.CO;2

Sobel, A. H., Nilsson, J., & Polvani, L. M. (2001). The weak temperature gradient approximation and balanced tropical moisture waves. *Journal of the Atmospheric Sciences*, *58*(23), 3650–3665. https://doi.org/10.1175/1520-0469(2001)058<3650:TWTGAA>2.0.CO;2

Stone, P. H., & Carlson, J. H. (1979). Atmospheric lapse rate regimes and their parameterization. *Journal of the Atmospheric Sciences*, *36*(3), 415–423. https://doi.org/10.1175/1520-0469(1979)036<0415:ALRRAT>2.0.CO;2

Taschetto, A. S., Rodrigues, R. R., Meehl, G. A., McGregor, S., & England, M. H. (2016). How sensitive are the Pacific-tropical North Atlantic teleconnections to the position and intensity of El Niño-related warming? *Climate Dynamics*, *46*(5-6), 1841–1860. https://doi.org/10.1007/s00382-015-2679-x

Vecchi, G. A., & Soden, B. J. (2007). Effect of remote sea surface temperature change on tropical cyclone potential intensity. *Nature*, *450*(7172), 1066–1070. https://doi.org/10.1038/nature06423

Vecchi, G. A., Swanson, K. L., & Soden, B. J. (2008). Whither hurricane activity? *Science*, *322*(5902), 687–689. https://doi.org/10.1126/science.1164396

Vincent, E. M., Lengaigne, M., Menkes, C. E., Jourdain, N. C., Marchesiello, P., & Madec, G. (2011). Interannual variability of the South Pacific Convergence Zone and implications for tropical cyclone genesis. *Climate Dynamics*, *36*(9-10), 1881–1896. https://doi.org/10.1007/s00382-009-0716-3

Wieners, C. E., Dijkstra, H. A., & de Ruijter, W. P. (2017). The influence of atmospheric convection on the interaction between the Indian Ocean and ENSO. *Journal of Climate*, *30*(24), 10,155–10,178. https://doi.org/10.1175/JCLI-D-17-0081.1

Williams, I. N., & Patricola, C. M. (2018). Diversity of ENSO events unified by convective threshold sea surface temperature: A nonlinear ENSO index. *Geophysical Research Letters*, *45*(17), 9236–9244. https://doi.org/10.1029/2018GL079203

Xie, P., & Arkin, P. A. (1997). Global precipitation: A 17-year monthly analysis based on gauge observations, satellite estimates, and numerical model outputs. *Bulletin of the American Meteorological Society*, *78*(11), 2539–2558. https://doi.org/10.1175/1520-0477(1997)078<2539:GPAYMA>2.0.CO;2

Xie, S. P., Deser, C., Vecchi, G. A., Ma, J., Teng, H., & Wittenberg, A. T. (2010). Global warming pattern formation: Sea surface temperature and rainfall. *Journal of Climate*, *23*(4), 966–986. https://doi.org/10.1175/2009JCLI3329.1

Xie, S. P., Hu, K., Hafner, J., Tokinaga, H., Du, Y., Huang, G., & Sampe, T. (2009). Indian Ocean capacitor effect on Indo-western Pacific climate during the summer following El Niño. *Journal of Climate*, *22*(3), 730–747. https://doi.org/10.1175/2008JCLI2544.1

References From the Supporting Information

Adames, Á. F., & Wallace, J. M. (2017). On the tropical atmospheric signature of El Niño. *Journal of the Atmospheric Sciences*, *74*(6), 1923–1939. https://doi.org/10.1175/JAS-D-16-0309.1

Bellenger, H., Guilyardi, É., Leloup, J., Lengaigne, M., & Vialard, J. (2014). ENSO representation in climate models: From CMIP3 to CMIP5. *Climate Dynamics*, *42*(7-8), 1999–2018. https://doi.org/10.1007/s00382-013-1783-z

Brown, J. N., Matear, R. J., Brown, J. R., & Katzfey, J. (2015). Precipitation projections in the tropical Pacific are sensitive to different types of SST bias adjustment. *Geophysical Research Letters*, *42*, 10–856. https://doi.org/10.1002/2015gl066184

Chen, C., Cane, M. A., Wittenberg, A. T., & Chen, D. (2017). ENSO in the CMIP5 simulations: Life cycles, diversity, and responses to climate change. *Journal of Climate*, *30*(2), 775–801. https://doi.org/10.1175/JCLI-D-15-0901.1

Chen, L., Li, T., Yu, Y., & Behera, S. K. (2017). A possible explanation for the divergent projection of ENSO amplitude change under global warming. *Climate Dynamics*, *49*(11-12), 3799–3811. https://doi.org/10.1007/s00382-017-3544-x

Collins, M., An, S. I., Cai, W., Ganachaud, A., Guilyardi, E., Jin, F. F., & Vecchi, G. (2010). The impact of global warming on the tropical Pacific Ocean and El Niño. *Nature Geoscience*, *3*(6), 391–397. https://doi.org/10.1038/ngeo868

Dee, D. P., Uppala, S. M., Simmons, A. J., Berrisford, P., Poli, P., Kobayashi, S., & Bechtold, P. (2011). The ERA-Interim reanalysis: Configuration and performance of the data assimilation system. *Quarterly Journal of the Royal Meteorological Society*, *137*(656), 553–597. https://doi.org/10.1002/qj.828

Fathrio, I., Iizuka, S., Manda, A., Kodama, Y.-M., Ishida, S., Moteki, Q., et al. (2017). Assessment of western Indian Ocean SST bias of CMIP5 models. *Journal of Geophysical Research, Oceans*, *122*(4), 3123–3140. https://doi.org/10.1002/2016JC012443

Ham, Y. G., & Kug, J. S. (2016). ENSO amplitude changes due to greenhouse warming in CMIP5: Role of mean tropical precipitation in the twentieth century. *Geophysical Research Letters*, *43*(1), 422–430. https://doi.org/10.1002/2015GL066864

Held, I. M., & Soden, B. J. (2006). Robust responses of the hydrological cycle to global warming. *Journal of Climate*, *19*(21), 5686–5699. https://doi.org/10.1175/JCLI3990.1

Huffman, G. J., Adler, R. F., Bolvin, D. T., & Gu, G. (2009). Improving the global precipitation record: GPCP version 2.1. *Geophysical Research Letters*, *36*, L17808. https://doi.org/10.1029/2009GL040000

Parvathi, V., Suresh, I., Lengaigne, M., Izumo, T., & Vialard, J. (2017). Robust projected weakening of winter monsoon winds over the Arabian Sea under climate change. *Geophysical Research Letters*, *44*(19), 9833–9843. https://doi.org/10.1002/2017GL075098

Rayner, N. A., Parker, D. E., Horton, E. B., Folland, C. K., Alexander, L. V., Row- ell, D. P., et al. (2003). Global analyses of sea surface temperature, sea ice, and night marine air temperature since the late nineteenth century. *Journal of Geophysical Research*, *108*(D14), 4407. https://doi.org/10.1029/2002JD002670

Richter, I., Xie, S. P., Behera, S. K., Doi, T., & Masumoto, Y. (2014). Equatorial Atlantic variability and its relation to mean state biases in CMIP5. *Climate Dynamics*, *42*(1-2), 171–188. https://doi.org/10.1007/s00382-012-1624-5

Wittenberg, A. T. (2009). Are historical records sufficient to constrain ENSO simulations? *Geophysical Research Letters*, *36*(12), L12702. https://doi.org/10.1029/2009GL038710

Yun, K. S., Yeh, S. W., & Ha, K. J. (2016). Inter-El Niño variability in CMIP5 models: Model deficiencies and future changes. *Journal of Geophysical Research-Atmospheres*, *121*(8), 3894–3906. https://doi.org/10.1002/2016JD024964

Zebiak, S. E. (1993), Air-sea interaction in the equatorial Atlantic region, *Journal of Climate*, *6*, 1567–1586. https://doi.org/10.1175/1520-0442(1993)006<1567:AIITEA>2.0.CO;2